Synchronized oscillations in Josephson junction arrays: The role of distributed coupling

A. B. Cawthorne, P. Barbara, S. V. Shitov,* and C. J. Lobb
Center for Superconductivity Research, Department of Physics, University of Maryland at College Park, College Park, Maryland 20742-4111

K. Wiesenfeld and A. Zangwill
School of Physics, Georgia Institute of Technology, Atlanta, Georgia 30332
(Received 25 February 1999)

We present experimental and theoretical results showing that the distributed electromagnetic environment of a Josephson junction array can cause the junctions in the array to synchronize. Based on our experimental results and our distributed array model, we find that an external load is not necessary for junction synchronization. Also, we show that the high-frequency performance of an array can be significantly better than the performance of a single isolated junction. [S0163-1829(99)01034-6]

Coupled nonlinear oscillators have been used to model a broad range of physical systems, including laser arrays,[1,2] coupled phase-locked loops,[3] and Josephson junction arrays.[4–8] Although the effects of coupling, including synchronization and phase locking, are easily observed, it is often very difficult to determine the mechanisms by which the coupling occurs. For Josephson junction arrays, recent progress in understanding nonlinear cooperative dynamics including order-disorder transitions[9] and collective resonance phenomena[10] has been based on lumped circuit models. We claim that the associated coupling mechanism cannot explain the success of the best performing arrays,[11–13] which are spatially distributed. Further, as arrays contain more junctions and operate at higher frequencies, the lumped description becomes increasingly inadequate.

When a Josephson junction is biased at a nonzero voltage, the supercurrent through the junction oscillates at a fundamental frequency given by $\nu_J = \langle V \rangle / \Phi_0 \approx \langle V \rangle 483$ GHz/mV, where $\langle V \rangle$ is the average dc voltage across the junction and Φ_0 is the flux quantum.[14] Although typical junctions can operate at frequencies of several hundred gigahertz, the power available from a single junction is not sufficient for most applications, necessitating arrays of junctions.[4–8,11,12] Since Josephson junctions are nonlinear oscillators, junctions in an array do not necessarily oscillate at the same frequency or in phase.

Most theories describing the synchronization and phase locking of junctions in a Josephson junction array use a lumped approach [shown in Fig. 1(a)]. These theories require feedback through an external load for phase locking.[4,15–17] Furthermore, the character of the load strongly influences the stability of the in-phase state.[15–17] Thus current theory predicts that identical arrays with substantially different loads should behave differently. Experiments by Benz and Booi have also suggested that the performance of an array of junctions will be limited by the characteristics of the single junctions in the array.[19,18]

Using the resistively capacitively inductively shunted junction (RCLSJ) model, and the method outlined in Refs. 20 and 8, we determined the parameters of a single isolated junction which has the same design as the junctions in our arrays.[8,20] Figure 2 shows the computed first-harmonic voltage amplitude of a junction with these parameters. Fig. 2 shows that the maximum voltage oscillation amplitude of a single junction occurs at about 150 GHz. According to Ref. 18, an array made from these junctions should have optimal performance near this frequency and poor performance above this frequency.

We next describe the design of three arrays. According to the previous discussion, the first two arrays should operate very differently. The third array, however, should have operation similar to the first. Measurements of these arrays will then be used to show that the theoretical predictions outlined above are inadequate.

Figure 3(a) shows a micrograph of a 10×10 array, which we will call a type-I array. It is 240 μm long and is connected to a detector junction through a 380-μm-long coupling capacitor. We use a detection scheme very similar to that used by Benz and Burroughs;[5] a schematic is shown in Fig. 3(c). Figure 3(b) shows a 5×10 array which has the same length as the 10×10 array, but is connected to the detector through a capacitor which is 90 μm long. We will call this a type-II array.

We will also discuss measurements of an array with the

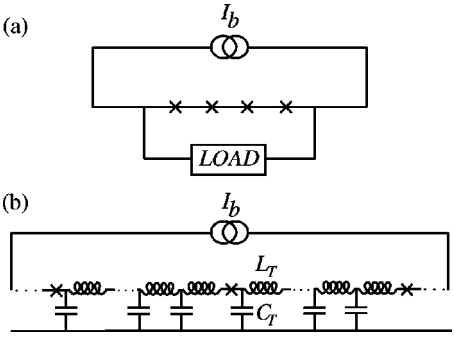

FIG. 1. (a) Lumped model of a one-dimensional Josephson junction array. Nonidentical junctions will not synchronize without a load. (b) Distributed model of a one-dimensional Josephson junction array, where each junction is connected to its neighbors by a short section of transmission line. Each junction is modeled by the RCLSJ model (inset of Fig. 2).

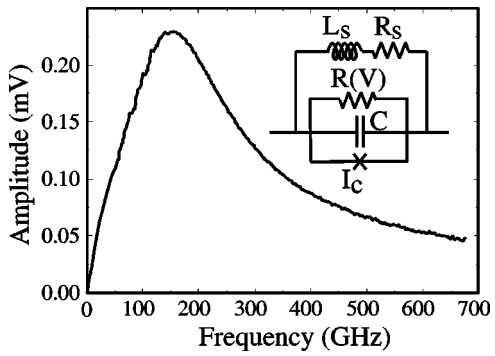

FIG. 2. Simulated first harmonic voltage amplitude of the individual junctions used in our arrays. The junction parameters are $I_c = 110\ \mu A$, $R_s = 1.06\ \Omega$, $\beta_C = 2\pi I_c R_s^2 C/\Phi_0 = 0.35$, and $\beta_L = 2\pi I_c L_s/\Phi_0 = 0.35$. The inset shows a schematic of the RCLSJ model.

same design as the array shown in Fig. 3(a). The ground plane of this type-III array, however, is *under* the array, rather than over the array as it is in Fig. 3. The distance between the junctions and the ground plane is about 0.2 μm when the ground plane is on the bottom, and 0.5 μm when the ground plane is on the top.

Because the coupling and the load are similar, standard lumped analysis predicts that type-I and type-III arrays should operate over roughly the same frequency range. In contrast, the load seen by the type-II array is substantially different from the load seen by the other arrays. The behavior of the type-II arrays should be different from that of the type-I or type-III arrays if a lumped model applies.[15–17]

To detect microwave output from the array, we measure the current-voltage characteristic of the detector junction. When enough power is present, Shapiro steps appear on the detector *I-V* curve, as shown in Fig. 4. For a given frequency ν, the step voltage (first step voltage labeled ''V_1'' in Fig. 4) is given by $V_n = n\Phi_0\nu$, where n is an integer. The widths of

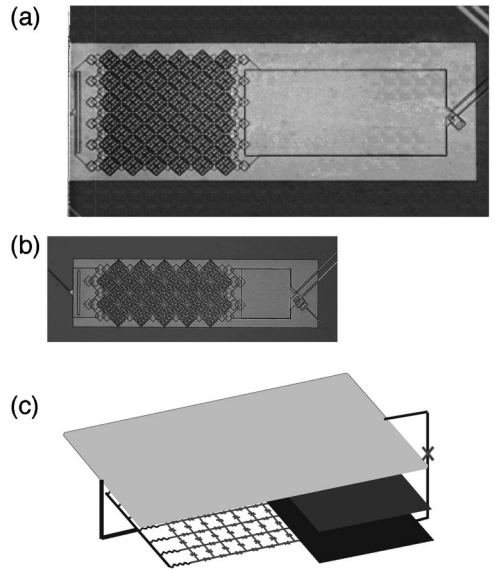

FIG. 3. (a) Micrograph of a 10×10 array which has a superconducting ground plane above the array (type I). (b) A 5×10 array which has a much smaller coupling circuit (type-II). (c) Schematic of the array and detector. The arrays are 240 μm long.

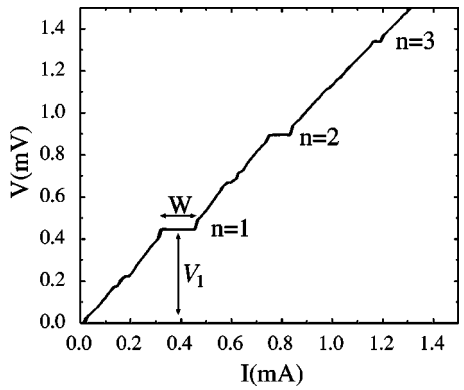

FIG. 4. Current-voltage characteristic of a detector junction when the array connected to the detector is operating at about 200 GHz. The step voltage V_1 is precisely related to the input frequency, and the step width is related to the input power.

the Shapiro steps (labeled ''*W*'' in Fig. 4) are related to the power coupled to the detector.[21]

Figure 5 shows the step width versus frequency for the first Shapiro step measured on the detector of each array. In this range of power, the step width increases as the power increases. The lumped analysis predicts that the type-I array data in Fig. 5(a) will differ from that of the type-II array shown in Fig. 5(b). Also, the type-I array should be similar to the type-III array, Fig. 5(c), since the junctions are the same and the loads are similar. In fact, we see that although the type-I and type-II arrays differ in overall power output, the frequency range for coherent output is the same. On the other hand, the type-III array, which has the ground plane on the bottom, operates at a much higher frequency than the type-I array, which has the ground plane on the top. Since all of the arrays use the same junctions, the characteristics of the individual junctions cannot explain these results. Also, the load does not strongly influence the operation of the array. Thus we see that current theory[4,15–18] does not adequately describe our arrays.

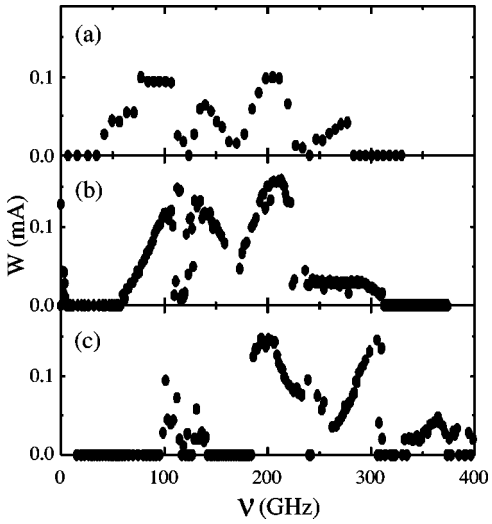

FIG. 5. Width of the first Shapiro step versus frequency for three array oscillators. (a) Type I 10×10 array with ground plane on top. (b) Type II 5×10 array with ground plane on top. (c) Type III 10×10 array with ground plane on bottom.

In our experiments, changing the coupling circuit has only a small effect on the performance of the arrays. On the other hand, changing the distance between the array and the ground plane has a significant effect. Because the distance between the array and the ground plane is much smaller than the array cell size (0.2 μm compared to 22 μm), the wiring connecting the junctions can be considered to be short transmission lines. Therefore we developed a model which describes a simplified series array of junctions embedded in a transmission line, shown schematically in Fig. 1(b).

The equations which describe this system are

$$I_b + I(x_j,t) - I_{sj} = C\frac{d^2\gamma_j}{dt^2} + \frac{1}{R(V_j)}\frac{d\gamma_j}{dt} + I_{cj}\sin(\gamma_j), \quad (1)$$

$$\frac{\hbar}{2e}\frac{d\gamma}{dt} = L_s\frac{dI_{sj}}{dt} + I_{sj}R_s, \quad (2)$$

$$V(x_j^+,t) - V(x_j^-,t) = -\frac{\hbar}{2e}\frac{d\gamma_j}{dt}, \quad (3)$$

$$\frac{\partial I(x,t)}{\partial x} = -C_T\frac{\partial V(x,t)}{\partial t}, \quad (4)$$

$$\frac{\partial V(x,t)}{\partial x} = -L_T\frac{\partial I(x,t)}{\partial t} - R_T I(x,t). \quad (5)$$

Equations (1)–(3) are valid at the junctions, and Eqs. (4) and (5) are valid in the regions connecting the junctions. In the above equations, $I(x,t)$ is the time-varying component of the current flowing in the lines at time t and position x, and $V(x,t)$ is the voltage. The phase difference of junction j is γ_j, and the current through the shunt branch of the jth junction is I_{sj}. The critical current of the jth junction is I_{cj}. The bias current in the array is I_b, and the position of the jth junction is x_j. The capacitance and inductance per unit length of the transmission lines are C_T and L_T, respectively. Dissipation in the transmission line is modeled by a resistance per unit length R_T.

In order to allow for numerical simulations, we have approximated two main aspects of our experimental arrays. First, the boundary conditions in our model are different from those in our experimental arrays. In the model, there is no ac current flowing at the ends of the array (i.e., there is no load). In our experimental arrays, there is a load (coupling capacitor and detector) connected to one end of the array and the other end of the array is shorted to the ground plane. When the oscillation frequency of the array is small enough that the lumped approach is appropriate, the lack of a load in the model will be very significant.[4,15–17] At higher frequencies, however, we can expect important aspects of the experiment to be correctly described by the model.

The second difference between our model and our experiments is that the model describes a one-dimensional array, and our experiments involve two-dimensoinal arrays. In the lumped analysis, it is often possible to reduce a two-dimensional array to an equivalent one-dimensional array.[22] Although transverse modes would make a similar simplification impossible for the distributed case, such modes are undesirable because they would lead to unlocking along the rows of the array. In fact, many important aspects of our experiments on two-dimensional arrays are reproduced by this simplified model.

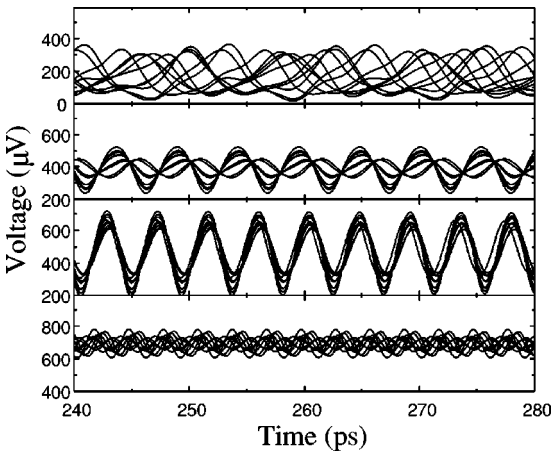

FIG. 6. Simulated voltage wave forms versus time at different values of the bias current for a ten junction type-III array with a $\pm 10\%$ spread in the critical currents and no load. (a) $I_b = 198$ μA (79 GHz), junctions unlocked, (b) $I_b = 385$ μA (190 GHz), junctions synchronized although the junctions at the ends of the array are out of phase, (c) $I_b = 473$ μA (231 GHz), junctions synchronized and all nearly in phase, (d) $I_b = 671$ μA (334 GHz), junctions unlocked.

Figure 6 shows the simulated voltage wave forms of each junction of a ten junction type-III array. We used $L_T = 0.052$ pH/μm and $C_T = 5.43$ fF/μm, which are estimated from the geometry of the type-III array, which has the ground plane on the bottom. (The estimated parameters for the type-I or -II array are $L_T = 0.11$ pH/μm and $C_T = 1.35$ fF/μm.) There is a $\pm 10\%$ uniform spread in the junction critical currents, and the initial conditions for the junction phases are chosen randomly.

Figure 6(a) shows that the junctions are not synchronized at low frequency. At frequencies from about 190–230 GHz, however, the junctions synchronize. Note that in Fig. 6(b), the junctions are synchronized in the sense that the junction voltages are all oscillating at the same frequency, even though all of the junction voltages are not in phase. Also note that the voltage amplitude is largest at about 230 GHz [Fig. 6(c)], corresponding to the junctions oscillating mostly in phase. Thus we see that the junctions in a disordered array can synchronize without an external load.

Because we do not model the detection circuit, we cannot directly compare the simulations and the experiment. We can, however, quantify the performance of the simulated array and compare the results to Fig. 5. To do this, we calculated the the average voltage $\langle V_{tot}\rangle$ across the junctions in the array, and from it calculated an average Josephson frequency $\nu_{Jav} = \langle V_{tot}\rangle / 10\Phi_0$. We then calculated the time-dependent voltage amplitude of the sinusoidal spatial modes $A_k(t)$ for $k_n = n\pi/L$. The voltage drop across a junction at position x_j is given by $v(x_j,t) = \Sigma A_k(t)\ \sin\ k_n x_j$. The Fourier amplitude of A_k at the frequency ν_{Jav} was then computed. A large amplitude implies phase and frequency locking of the oscillations of each junction.

The results for k_1, k_2, and k_3 are shown in Fig. 7 for arrays with both the ground plane on top (type I and II) and

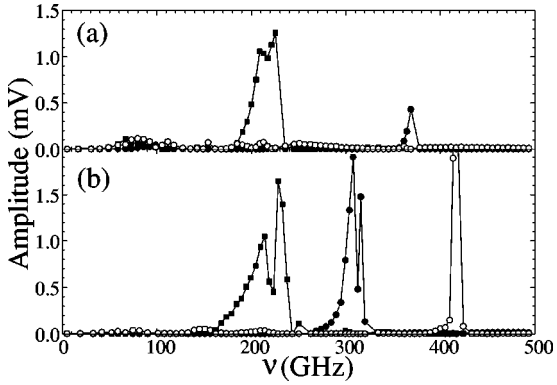

FIG. 7. Simulated Fourier voltage amplitudes of the lowest three spatial modes in ten junction arrays. The solid squares represent the k_1 mode, the solid circles are the k_2 mode, and the open circles are the k_3 mode. (a) Type-I and -II arrays, ground plane on top. (b) Type-III array, ground plane on bottom.

on bottom (type III). When the ground plane is moved from the top to the bottom of the array, the k_2 mode moves down in frequency while the k_1 mode stays at around 200 GHz. The k_3 mode has a peak at about 410 GHz in Fig. 7(b) and is either at a high frequency (greater than 500 GHz) or is not present in Fig. 7(a).

Comparison of Fig. 7(a) with Figs. 4(a) and 4(b) shows that although the lower-frequency (around 100 GHz) response in the experiment is not as strong in the simulation, the response at 200 GHz is reproduced. (It is likely that the low-frequency coupling in the experimental arrays comes from the load,[15–17] which we do not simulate.) The simulation also correctly predicts that the output will be small above the band at 200 GHz. Comparison of Fig. 7(b) with Fig. 4(c) shows that the simulation predicts the increased power at around 300 GHz. The simulation also predicts very small output at frequencies below the peak at 200 GHz. We note here that we expect the peak at 410 GHz to be strongly attenuated by the coupling circuit in the experimental array.

We have introduced a distributed Josephson-junction array oscillator model which correctly predicts many features of our experiments. First, our model shows that the transmission lines connecting the junctions synchronize the array: an external load is not required. This explains why drastically changing the load of our experimental arrays did not greatly alter their operating frequency range. Second, our model correctly predicts that it is possible to have coherent output at frequencies well above the frequency at which the single-junction output is largest. In fact, both the measurements and simulations of the type-III array showed very small output at this frequency. Third, our results indicate that decreasing the distance from the ground plane to the array can raise the operating frequency range of the array. As future arrays are pushed to higher power (more junctions) and higher frequency, the distributed description may provide the necessary theoretical tools to design very large Josephson junction array oscillators.

This work was supported by the AFOSR under Contract No. F49620-98-1-0072 and by the Center for Superconductivity Research at the University of Maryland. We would also like to thank T. M. Antonsen and E. Ott for useful discussions.

*Present address: Institute for Radio Engineering and Electronics, Russian Academy of Sciences, Mokhovaya 11, Moscow 103907, Russia.

[1] K. S. Thornburg, M. Moller, R. Roy, T. W. Carr, R. D. Li, and T. Erneux, Phys. Rev. E **55**, 3865 (1997).
[2] H. H. Winful, Phys. Rev. A **46**, 6093 (1992).
[3] J. J. Lynch and R. York, IEEE Microwave Guid. Wave Lett. **5**, 213 (1995).
[4] A. K. Jain, K. K. Likharev, J. E. Lukens, and J. E. Sauvageau, Phys. Rep. **109**, 309 (1984).
[5] S. P. Benz and C. J. Burroughs, Appl. Phys. Lett. **58**, 2162 (1991).
[6] K. Wiesenfeld, S. P. Benz, and P. A. A. Booi, J. Appl. Phys. **76**, 3835 (1994).
[7] A. B. Cawthorne, P. Barbara, and C. J. Lobb, IEEE Trans. Appl. Supercond. **7**, 3403 (1997).
[8] A. B. Cawthorne, Ph.D. dissertation, University of Maryland, 1998, available in electronic form at http://complex.umd.edu/fred or by email request to fcawth@squid.umd.edu
[9] K. Wiesenfeld, P. Colet, and S. H. Strogatz, Phys. Rev. Lett. **76**, 404 (1996).
[10] S. Watanabe, S. H. Strogatz, H. S. J. van der Zant, and T. P. Orlando, Phys. Rev. Lett. **74**, 379 (1995).
[11] S. Han, B. Bi, W. Zhang, and J. E. Lukens, Appl. Phys. Lett. **64**, 1424 (1994).
[12] P. A. A. Booi and S. P. Benz, Appl. Phys. Lett. **68**, 3799 (1996).
[13] P. Barbara, A. B. Cawthorne, S. V. Shitov, and C. J. Lobb, Phys. Rev. Lett. **82**, 1963 (1999).
[14] B. D. Josephson, Phys. Lett. **1**, 251 (1962).
[15] P. Hadley, M. R. Beasley, and K. Wiesenfeld, Appl. Phys. Lett. **52**, 1619 (1988).
[16] P. Hadley, M. R. Beasley, and K. Wiesenfeld, Phys. Rev. B **38**, 8712 (1988).
[17] P. Hadley, Ph.D. thesis, Stanford University, 1989.
[18] P. A. A. Booi and S. P. Benz, IEEE Trans. Appl. Supercond. **5**, 2899 (1995).
[19] In particular, the junction-shunt LC resonance frequency is said to limit the high-frequency operation of arrays.
[20] A. B. Cawthorne, C. B. Whan, and C. J. Lobb, J. Appl. Phys. **84**, 1126 (1998).
[21] S. Shapiro, Phys. Rev. Lett. **11**, 80 (1963).
[22] R. L. Kautz, IEEE Trans. Appl. Supercond. **5**, 2702 (1995).